Dalton Transactions

ROYAL SOCIETY OF CHEMISTRY

PAPER

View Article Online
View Journal | View Issue

Cite this: *Dalton Trans.*, 2021, **50**, 16084

Hypercoordinated eka-tin materials with dangling aryl-methoxy and -methylthio ligands exhibiting intramolecular secondary bonding and aryl bond stabilization in reactions with organotin chlorides†

Alfredo Ornelas, Renzo Arias-Ugarte, Alejandro J. Metta-Magaña, Hemant K. Sharma and Keith H. Pannell *

Received 26th August 2021,
Accepted 13th October 2021

DOI: 10.1039/d1dt02781f

rsc.li/dalton

The syntheses of $[2\text{-}(CH_3ECH_2)C_6H_4]PbPh_{3-n}Cl_n$, ($n$ = 0, E = O (**4**), E = S (**5**); n = 1, E = O (**6**), E = S (**7**); n = 2, E = O (**8**), are described. NMR and single crystal data illustrate significant Pb···E interactions increasing as n progresses from 0 to 2. The Pb···E interactions stabilize the Pb–aryl bonding to the extent that the reactions of **4** and **5** with Me_2SnCl_2 result in interchange of a Ph group and Cl to produce **6** and **7**, respectively, together with $Me_2PhSnCl$.

Introduction

The study and development of organolead chemistry can be thought to begin with the report of a series of ethyllead materials by Lowig in 1853,[1,2] and perhaps the most significant discovery in the field was that of Midgley and Boyd in 1922 revealing the excellent "anti-knock" properties of tetraethyllead, $PbEt_4$.[3] However, following the widespread distribution of lead materials from automobile exhausts, and its incorporation into the human body and the resulting negative health impacts, tetraethyllead has been phased out and banned in most countries.

The majority of organolead compounds studied are in the form of R_4Pb, R_3PbX, R_2PbX_2 or $RPbX_3$ where R is an organic moiety and X an electronegative species.[4] Such systems exhibit interesting chemistry, including group transfer from R_4Pb to aldehydes,[5,6] stereoselective reactions,[7,8] carbon–carbon bond forming reactions,[9–11] and aryl/alkyl transfer reactions to tin and related main group elements.[12]

Whereas the homoleptic lead(IV) halides, PbX_4 (X = F, Cl, Br, I), are unstable and transform to the corresponding lead(II) halides; the organolead halides $R_{4-n}PbX_n$ (R = alkyl or aryl, n = 0–3) exhibit enhanced stability.[13] Aryllead halides are more stable than their alkyl counterparts.[14]

A characteristic of many of the main group elements that provides enhanced chemical reactivity is their capacity to act as Lewis acids. This is particularly interesting within the elements of group 14, with a classic example being the hydrolytic reactivity of chlorosilanes when compared to their carbon analogs. Despite the significantly greater Si–Cl bond strength (calculated bond dissociation energy Si–Cl = 448.4, C–Cl = 338.1 kJ mol^{-1}),[15] the chlorosilanes can be explosively reactive with water whereas related carbon materials are insoluble and effectively non-reactive. This latter property is responsible for the environmental accumulation of organohalides in fatty tissue of marine animals and further up the food chain.[16] The presence of low energy reaction pathways involving the direct formation of penta(hexa)coordinate transients that result in ready displacement of the chloride ion is responsible for such displacement reactions. The interaction between an electron-pair donating moiety and a group 14 metal or metalloid acting as a Lewis acid has been defined as a tetrel bond.[17a,b]

An excellent review of hypercoordinate group 14 compounds has been published,[18a] and many examples of such organotin compounds, formed by strong inter- and intra-molecular acid–base interactions both in the solid state and in solution, have been reported.[18] Some examples relevant to our study are illustrated in Fig. 1.[19–23]

Intramolecular secondary bonding can impact both the chemical and biological activity of the resulting materials. For example, $(CH_3SCH_2CH_2CH_2)_2SnCl_2$, **3b**, is relatively inert toward human natural killer cells when compared to the related di(n-butyl)tin dichloride, $(CH_3CH_2CH_2CH_2)_2SnCl_2$, but maintains the capacity to act as an efficient esterification catalyst.[23a] The same material has also been demonstrated as an

Department of Chemistry, The University of Texas at El Paso, El Paso, TX 79968-0513, USA. E-mail: kpannell@utep.edu

† Electronic supplementary information (ESI) available: ^{207}Pb and ^{119}Sn monitoring of the phenyl group transfer reactions. CCDC 2087426–2087430. For ESI and crystallographic data in CIF or other electronic format see DOI: 10.1039/d1dt02781f

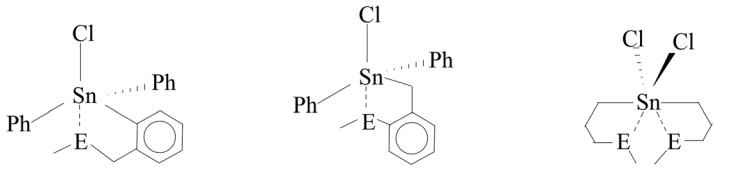

E = O (**1a**); MeN (**1b**) E = O (**2a**); S (**2b**) E= O (**3a**); S (**3b**)

Fig. 1 Typical intramolecular hypercoordinated organotin chlorides: **1**, E = O (**a**);[19] E = MeN (**b**);[20] **2**, E = O (**a**),[21] E = S (**b**);[21] **3**, E = O (**a**),[22] E = S (**b**).[23]

excellent therapeutic reagent against *Trypanosoma cruzi* infection.[23b]

To date, there are relatively few examples of the corresponding lead-based analogs exhibiting such intramolecular secondary bonding. The most notable examples are those reported by the Silvestru group, [2-(Me_2NCH_2)C_6H_4]$PbPh_2R$, R = Ph, Cl,[24] and ourselves, [2-(MeO)$C_6H_4CH_2$]$PbPh_2R$, R = Ph, Cl.[25] We now report the synthesis and structural characterization of simple organoleads containing dangling donor atoms (E): [2-(CH_3ECH_2)C_6H_4]$PbPh_3$, E = O (**4**), E = S (**5**); their chloro-substituted derivatives, [2-(CH_3ECH_2)C_6H_4]$PbPh_2Cl$ (E = O, (**6**), E = S, (**7**) and [2-(CH_3ECH_2)C_6H_4]$PbPhCl_2$, E = O, (**8**). Structural characterization of the new materials demonstrates significant E···Pb intramolecular bonding and treatment of **4**, **5**, **6** and **7** with HCl, or Me_2SnCl_2, results in cleavage of the unsubstituted Pb–Ph bond, demonstrating the relative stability of the [2-(CH_3ECH_2)C_6H_4] aryl–lead bond (Fig. 2).

Experimental

Materials and methods

All manipulations were carried out under a nitrogen or argon atmosphere using Schlenk or vacuum line techniques. Solvents were used subsequent to drying by normal techniques. NMR spectra were recorded on a 300 MHz Bruker spectrometer in $CDCl_3$ (Cambridge Isotopes Laboratory Inc.) or $(CD_3)_2CO$ (Aldrich). Mass spectrometry was performed on a high resolution JEOL Accu TOF mass spectrometer using an electrospray ionization (ESI) source and direct analysis in real time (DART). Sodium methoxide and *n*-BuLi were purchased from Aldrich; 2-bromobenzyl bromide and HCl/Et_2O were purchased from Sigma-Aldrich; Ph_3PbCl was obtained from CHEM Cruz; Me_2SnCl_2 was purchased from Gelest Inc.; elemental analyses were performed by Galbraith Laboratories. Single crystal X-ray data were collected using three different diffractometers: Bruker Apex CCD, Bruker Quest Photon, and Bruker Venture Duo Photon, using APEX3 for the refinement and solution of the crystal structures. All solutions containing Pb materials were appropriately disposed of *via* the University Environmental Health and Safety Division.

Synthesis of [2-(methoxymethyl)phenyl]triphenylplumbane (4)

To a hexane (80 mL) solution of 1-bromo-2-(methoxymethyl) benzene (1.00 g, 4.98 mmol) in a 250 mL Schlenk flask cooled to −78 °C, was added dropwise a solution of *n*-BuLi (3.11 mL, 1.6 M, 5.0 mmol).[18e] The stirred reaction mixture was permitted to warm to room temperature, and after ~30 min a white precipitate was clearly observed. The reaction was cooled once again to −78 °C and a 25 mL THF solution of triphenyllead chloride **12** (2.12 g, 4.5 mmol, assuming 90% initial lithiation) was added dropwise. The reaction was stirred overnight at room temperature. The resulting solution was concentrated under vacuum to about 50 mL and then filtered using a fritted funnel to remove unwanted insoluble by-products. Removal of the solvent resulted in an oily compound which was precipitated by addition of 50 mL of anhydrous hexanes under sonication to form a white precipitate. The hexanes were removed by decantation and the process was repeated to wash the resulting precipitate. The resulting white solid compound was dried completely under vacuum and single crystals were obtained from a hexanes/dichloromethane solution, 1.92 g, 3.44 mmol, 77% yield based upon Ph_3PbCl used. ^1H NMR (300 MHz, $CDCl_3$, δ, ppm) 7.75–7.21 (m, 19H, Ar–H), 4.30

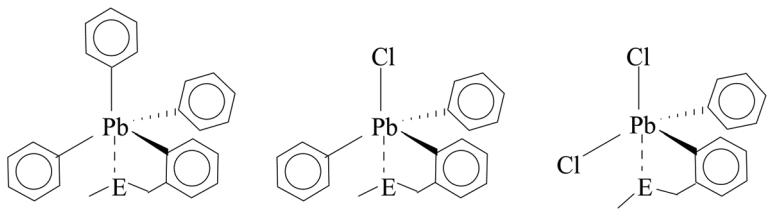

E = O (**4**); S (**5**) E = O (**6**); S (**7**) E = O (**8**)

Fig. 2 New organoleads containing dangling O and S ligands.

(CH_2), 2.85 (CH_3). ^{13}C NMR (75.4 MHz, $CDCl_3$, δ, ppm) 152.0, 145.1, 138.5, 137.7, 130.0, 129.4, 128.7, 128.6, 128.4, 128.2, 76.4, 57.7. ^{207}Pb NMR (63 MHz, $CDCl_3$, δ, ppm) −176.3. Elemental analysis (%) calcd for $C_{26}H_{24}OPb$ (559.68): C 55.80, H 4.32. Found: C 55.71, H 4.19; ESI-DART-MS m/z $[M - C_6H_5]^+$ calcd 483.1202 obs. 483.1209 (100%). m/z $[M - C_8H_9O]^+$ calcd 439.0940 obs. 439.0999 (32%).

Synthesis of [2-(methylthiomethyl)phenyl]triphenylplumbane (5)

This synthesis was carried out following the same procedure and ratios as the production of **4**, but using 1-bromo-2-(methylthiomethyl)benzene.[19] This reaction is slower than that with the oxygen analog, taking approximately 3 h. The crystalline product was obtained from a hexanes/dichloromethane solution in 70% yield. ^{1}H NMR (300 MHz, $CDCl_3$, δ, ppm) 7.77–7.17, 3.58, 1.62. ^{13}C NMR (75.4 MHz, $CDCl_3$, δ, ppm) 151.7, 145.2, 138.7, 137.7, 131.0, 130.6, 129.5, 128.7, 128.5, 127.8, 41.8, 14.9. ^{207}Pb NMR (63 MHz, $CDCl_3$, δ, ppm) −191.3. Elemental analysis, (%) calcd for $C_{26}H_{24}SPb$ (575.73): C 54.24, H 4.20. Found: C 53.34, H 4.10. Found: C 53.34, H 4.10; ESI-DART-MS m/z $[M - C_6H_5]^+$ calcd 499.0974 obs. 499.0972 (100%). m/z $[M - C_8H_9S]^+$ calcd 439.0940 obs. 439.0997 (21%).

Synthesis of chloro[2-(methoxymethyl)phenyl] diphenylplumbane (6)

An NMR tube was charged with **4** (0.25 g, 0.45 mmol) dissolved in $CDCl_3$ (0.60 mL) and flushed with nitrogen. The tube was placed in an acetone/liquid nitrogen bath at −25 °C for 30 minutes and a solution of HCl/Et_2O (1 M, 0.45 ml) (previously cooled to −25 °C) was added dropwise and mixed manually whence the solution immediately turns pale yellow. The mixture was left to react at −25 °C for a total of 3 h and monitoring by ^{207}Pb NMR spectroscopy demonstrated that the starting material (−176.3 ppm) was completely consumed and a new resonance had appeared at −49.5 ppm. The NMR tube was opened, and the solution was filtered through a acrodisc filter, and concentrated under vacuum to obtain an off-yellow crude solid which was dissolved in dichloromethane and crystallized by liquid–liquid diffusion using hexanes as the precipitating solvent. After filtration the product was recrystallized from a hexanes/dichloromethane solution to yield **6** in 90% yield (0.21 g). ^{1}H NMR (300 MHz, $CDCl_3$, δ, ppm) 8.42, 7.78, 7.59–7.26, 4.69, 3.22. ^{13}C NMR (75.4 MHz, $CDCl_3$, δ, ppm) 158.2, 152.2, 142.7, 137.9, 136.0, 130.2, 129.7, 129.6, 129.4, 127.0, 75.2, 58.9. ^{207}Pb NMR (63 MHz, $CDCl_3$, δ, ppm) −49.5. ESI-DART-MS m/z $[M - Cl]^+$ calcd 483.1202 obs. 483.1054 (75%).

Synthesis of chloro[2-(methylthiomethyl)phenyl] diphenylplumbane (7)

This reaction was carried out using the above procedure and ratios as for the synthesis of **6**. Chlorination of the thio-plumbane derivative **5** was relatively slower than its oxygen analog, 5 h at −25 °C. After filtering and removal of the solvent, a white solid was obtained and recrystallized as described previously to yield **7** in 87% (0.24 g) yield. ^{1}H NMR (300 MHz, $CDCl_3$, δ, ppm) 8.50, 7.90, 7.72–7.31, 3.80, 1.66. ^{13}C NMR (75.4 MHz, $CDCl_3$, δ, ppm) 157.8, 156.8, 141.5, 138.6, 136.2, 131.6, 130.3, 129.6, 129.5, 129.4, 38.9, 13.74. ^{207}Pb NMR (63 MHz, $CDCl_3$, δ, ppm) −46.5. ESI-DART-MS m/z $[M - Cl]^+$ calcd 499.0974 obs. 499.0822 (100%). m/z $[M - Ph]^+$ calcd 457.0271 obs. 457.0164 (23%). Elemental analysis, (%) calcd for $C_{20}H_{19}ClSPb$ (534.08): C 45.0, 3.39. Found: C 44.91, H 3.58.

Synthesis of dichloro[2-(methoxymethyl)phenyl] phenylplumbane (8)

An NMR tube was charged with a 0.6 mL $CDCl_3$ solution of **6** (0.10 g, 0.19 mmol). The solution was cooled to −25 °C for 30 min and a previously cooled solution of HCl in Et_2O (1 M, 0.19 mL) was added slowly. A pale-yellow precipitate was observed immediately. The reaction was left at −25 °C for 2 h when the starting material was finally consumed as indicated by ^{207}Pb NMR spectroscopy. No new ^{207}Pb resonances were observed in the $CDCl_3$ solution of the crude reaction, therefore the precipitate was filtered and washed with a cold $CHCl_3$/hexanes 2/1 solution followed by drying under vacuum to yield a pale yellow solid compound. Single crystals were produced from a boiling solution of acetone slowly cooled to 4 °C to yield **8** in 75% yield (0.07 g). ^{1}H NMR (300 MHz, $CDCl_3$, δ, ppm); 8.06 1H, 7.71–7.26, 4.82, 3.80; ^{13}C NMR (75.4 MHz, $(CD_3)_2CO$, δ, ppm) 164.36, 140.44, 134.26, 134.09, 133.84, 130.54, 130.45, 130.11, 129.68, 128.07, 73.06, 58.61; ^{207}Pb NMR (63 MHz, $(CD_3)_2CO$, δ, ppm) −66.0.

Reaction between [2-(methoxymethyl)phenyl] triphenylplumbane (4) and Me_2SnCl_2

An NMR tube was charged with a 0.6 mL $CDCl_3$ solution of **4** (0.05 g, 0.09 mmol) and Me_2SnCl_2 (0.02 g, 0.09 mmol). The tube was flushed with argon and sealed, covered with aluminum foil to protect it from light and placed in a 50 °C oil bath. Progress of the reaction was monitored by ^{207}Pb and ^{119}Sn NMR spectroscopy where the starting materials (−176.3 ppm, ^{207}Pb and +141 ppm, ^{119}Sn NMR) slowly disappeared to give new data (−48.9 ppm, ^{207}Pb, and 98.5 ppm, ^{119}Sn). These NMR data are consistent with products obtained by selective transfer of one phenyl group from lead to tin and a chlorine from tin to lead, *i.e.* **6** and the previously reported $Me_2PhSnCl$.[12,26a] An alternative possible product, chlorotriphenyllead **12**, is known to have a ^{207}Pb chemical shift of +33 ppm in $CDCl_3$.[26b] The reaction was slow, and it took a total of 90 h for all the starting materials to be transformed to give a quantitative yield by NMR.

Reaction between [2-(methylthiomethyl)phenyl] triphenylplumbane (5) and Me_2SnCl_2

This reaction was carried out following the same procedure and molar ratios as the reaction between Me_2SnCl_2 and **4** presented above. The reaction was monitored by ^{207}Pb NMR spectroscopy and a clean transformation from the starting material **5** −191.3 ppm was observed to yield the product **7** at −46.5 ppm along with the expected coproduct $Me_2PhSnCl$ over a period of 108 h. The reaction was quantitative based upon the NMR spectral analysis.

Results and discussion

Synthesis and characterization of $[2\text{-}(MeOECH_2)C_6H_4]Ph_3Pb$, E = O (4), E = S (5)

The methoxy- and methylthio- derivatives **4** and **5** were synthesized in good yield (>70%) from the reaction of 1-bromo-2-(methoxymethyl)benzene or 1-bromo-2-(methylthiomethyl) benzene with *n*-BuLi, to make the transient aryllithium (ArLi) *in situ*, followed by the addition of triphenyllead chloride (eqn (1)). This is the same methodology used by the Silvestru group for the formation of the closely related NMe_2 dangling arm organolead product $[2\text{-}(Me_2NCH_2)C_6H_4]PbPh_3$.[24] Both products were isolated as air-stable, mildly light sensitive solids, soluble in dichloromethane, chloroform, ethyl acetate, and THF.

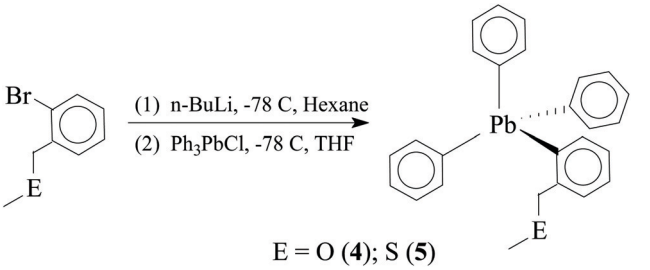

(1)

The ^1H and ^{13}C NMR spectral properties of both **4** and **5**, presented in the Experimental section, are in accord with their structural assignment, and the substituted aryl group data are similar to those of the parent $PhCH_2EMe$ compounds. However, the CH_2 and CH_3 ^1H resonances at 4.30 & 2.85 ppm (**4**) and 3.58 & 1.62 ppm (**5**) while similar to the parent ^1H resonances at 4.4 ppm & 3.3 ppm (E = O) and 3.6 ppm & 2.0 ppm (E = S), do exhibit an upfield shift of the CH_3 resonances. Inspection of the ^{13}C NMR data reflect a similar pattern.

The ^{207}Pb resonances at −176.3 ppm (**4**) and −191.3 ppm (**5**) are comparable to that of Ph_4Pb, a similar tetra-aryl substituted material without the dangling ligand moiety, which is reported to occur at −179.0 ppm.[26] The absence of any distinct chemical shift change suggesting little or no Pb···E interactions in solution, although it appear that the S atom have a larger impact.

The solid state single crystal structures of **4** and **5** are presented in Fig. 3. Both molecules crystallized in $P\bar{1}$, with two independent molecules present in the crystal structure. The intramolecular Pb···E distances are 2.998(2) & 3.151(5) Å (E = O, **4**), and 3.681(2) & 3.787(2) Å (E = S, **5**) representing 85 and 89% of the ΣvdW(Pb + O) radii, and 96 and 99% of the ΣvdW (Pb + S) radii. These data suggest a greater oxo-philicity of the central Pb metal, and indeed represent an unexpectedly strong Pb···O interaction in the relatively non-polarized lead(IV) species. However, this interaction does not reflect itself in the ^{207}Pb NMR data noted above and is thus a predominantly solid state phenomenon. Additionally, the disorder in the orientation of O in the structure of **4** in which one conformation exhibits a long Pb···O of 4.572(6) Å (129% of ΣvdW(Pb···O)) suggests that these data may also be impacted by some crystal packing issues.

The interactions of Pb with O and S do have a clear impact on both **4** and **5** with respect to the tetrahedral geometry that may be expected for a tetra-aryl lead material. In the case of **4**, we found two conformers in the asymmetric unit, with one of them having the oxygen disordered over two positions. These two conformers have different Td% (83% and 65%), while the conformer with the shortest contact has a 72% Td character, resulting in a weighted average of 73%. For the corresponding

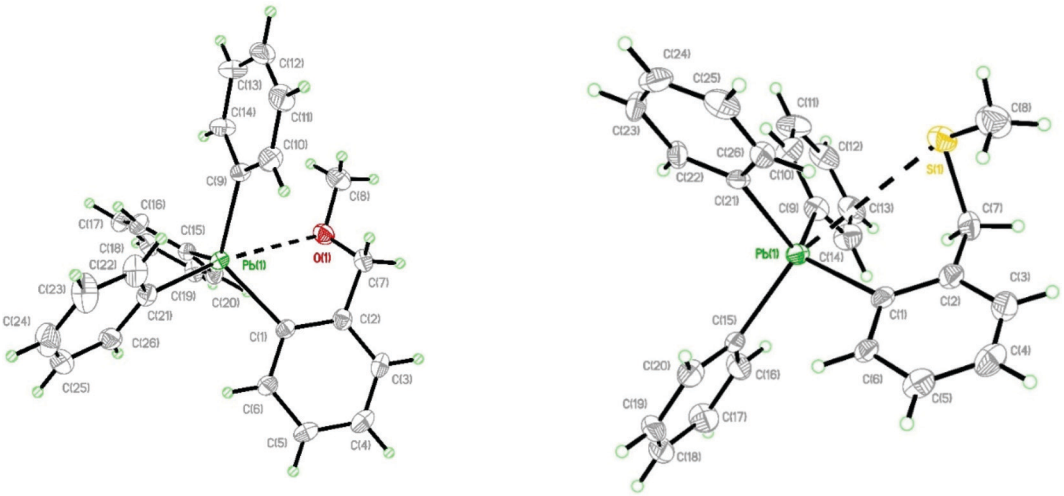

Fig. 3 Crystal structure of **4** (left, CCDC = 2087429†) and **5** (right, CCDC = 2087428†); only the conformer with the shortest contact is being shown at 50% of probability level for each one. Selected bond lengths (Å) and angles (°): **4**, Pb1–O1 = 2.998(2), O1–Pb1–C21 = 168.1(1), Pb1–O1–C7 = 96.5(2); **5**, S1–Pb1 = 3.681(2); S1–Pb1–C15 = 163.7(2), Pb1–S1–C7 = 69.7(2).

conformers of **5** the values are 58 and 74%, with a weighted average of 66%.

Synthesis and characterization of $[2\text{-}(Me_2ECH_2)C_6H_4]PbPh_2Cl$, E = O (6), E = S (7)

The initial syntheses of the mono-chloro-substituted lead compounds **6** and **7** were accomplished by simple treatment of the triphenyllead compounds **4** and **5** with an equimolar amount of HCl/Et_2O (Scheme 1).[24] At room temperature the reactions were almost instantaneous as observed by the consumption of the starting material by ^{207}Pb NMR spectroscopic monitoring. We observed the formation of two products in each reaction, the desired compounds **6** or **7** and Ph_3PbCl, in the ratio of 70 : 30. However, performing these reactions at −25 °C resulted in the cleavage of the phenyl group exclusively and **6** and **7** were obtained in high yield, ~90%. These results indicate that, however weak the Pb···E intramolecular interaction in **4** and **5**, it is significant enough to have an impact upon their chemistry and imparts a stability to the dangling-arm aryl–Pb bond.

The ^1H NMR spectra of **6** and **7**, for both the CH_2 and CH_3 groups at 4.69 ppm & 3.22 ppm (E = O) and 3.80 & 1.66 ppm (E = S), respectively, exhibit downfield shifts compared to **4** and **5**, a direct result of the introduction of the electronegative Cl atom bonded to lead. The related data for ^{13}C NMR, reported in the Experimental section, demonstrate no significant pattern. The ^{207}Pb NMR resonances for **6** and **7** at −49.5 ppm (**6**) and −46.5 ppm (**7**) exhibit a significant downfield shift compared to both **4** and **5** respectively (126.8 and 144.8 ppm) but a pronounced upfield shift ~80 ppm when compared to Ph_3PbCl (33.0 ppm). Such data indicate a significant intramolecular Pb···E interaction in solution, as expected by the increased Lewis acidity at the metal center due to replacement of a phenyl group by a halogen. For example, the 5-coordinate Ph_3PbCl·pyridine complex reported to exhibits a ^{207}Pb resonance at −174.0 ppm,[26] or −200 ppm,[27] dependent upon the ratios of the organolead and pyridine. The augmentation of the Pb···E secondary bonding is seen by the single crystal structures of **6** and **7** (Fig. 4).

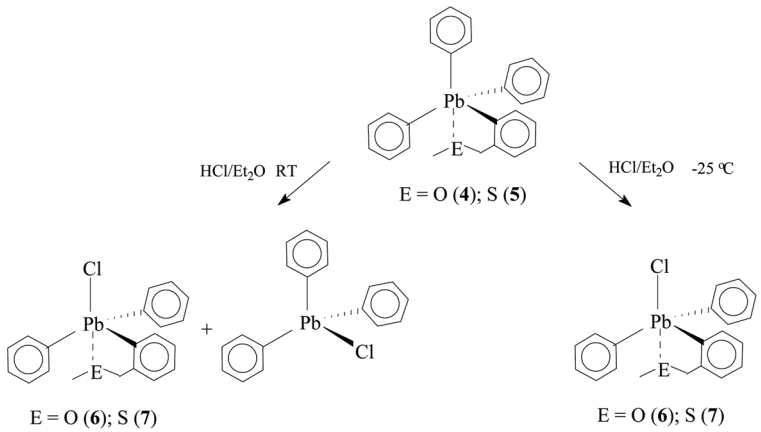

Scheme 1 Synthesis of **6** and **7** illustrating the impact of temperature on aryl substitution.

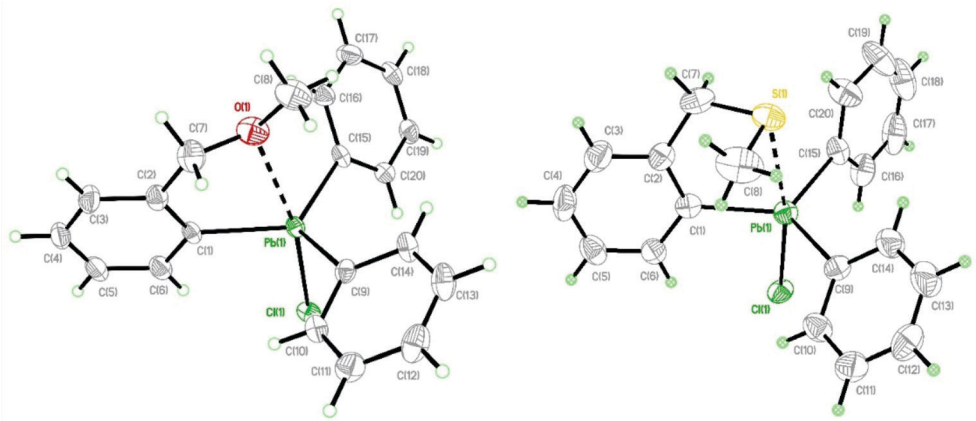

Fig. 4 ORTEP rendering of structures for **6** (CCDC = 2087430†) and **7** (CCDC = 2087426†) at 50% and 35% of probability level, respectively. Selected bond lengths (Å) and angles (°): **6**, O1–Pb1 = 2.618(3); Pb1–Cl1 = 2.555(1), O1–Pb1–Cl1 = 167.2(1), O1–Pb1–C1 = 70.8(2), O1–Pb1–C15 = 86.6(2), O1–Pb1–C9 = 88.9(1); **7**, S(1)–Pb(1) = 3.039(2); Pb(1)–Cl(1) = 2.599(2); S1–Pb1–Cl1 = 169.5(1), C7–S1–Pb1 = 85.5(3), S1–Pb1–C1 = 74.8(2), S1–Pb1–C9 = 85.1(2), S1–Pb1–C15 = 90.7(2).

In both compounds there is a significant Pb···E bonding with a *trans* type orientation with respect to the chlorine atom. The Pb···E contact distances are reduced significantly to 2.614(4) and 3.039(2) Å for **6** and **7**, respectively, representing 74% and 80% of corresponding ΣvdW radii. Relatedly, the TBP character is increased as expected to 82 and 87% of the TBP character.

The *trans*-effect, as exhibited by the impact of the O and S bonding on the Pb–Cl bond distance is notable;[4] with values of 2.552(1) Å (**6**) and 2.599(2) Å (**7**), both significantly shorter than the Pb–Cl bond of 2.612(5) Å reported for the tetrahedral monomeric Mes_3PbCl,[28] and for the distorted TBP polymeric structures of Ph_3PbCl, 2.71 Å,[29] and Me_3PbCl, 2.814 and 2.764 Å.[30] Similar shortening of the Sn–Cl bond has been observed for the organotin compounds $RSnPh_2Cl$, R = 2-(MeE)$C_6H_4CH_2$ (E = O, S)[21] and the isomeric R = 2-$(MeOCH_2)C_6H_4$ (E = O).[18e] Interestingly no significant shortening of the Pb–Cl bond length was observed for $[2\text{-}(Me_2NCH_2)C_6H_4]PbPh_2Cl$.[24]

Synthesis and characterization of $[2\text{-}(MeOCH_2)C_6H_4]PbPhCl_2$, (8)

The dichloro-lead compound **8** was readily obtained by treatment of **6** with the HCl/Et_2O reagent, again using the low temperature route (reaction (2)). Attempts to directly convert **4** to **8** using 2 equivalents of HCl/Et_2O were unsuccessful and led to an insoluble solid product. Also in this chemistry, in our hands, attempts to transform the thio material **7** to a dichloro product failed.

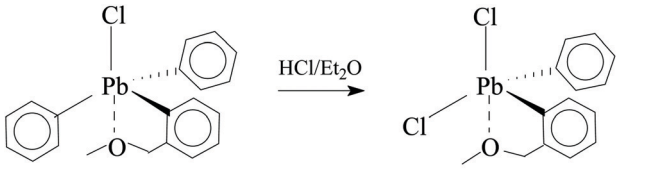

6 **8** (2)

Once again, the HCl conversion of **6** to **8** illustrates the extra resistance to cleavage of the aryl group containing the dangling arm O atom. The ^1H and ^{13}C NMR data associated with **8** are in accord with the structure observed. The ^{207}Pb NMR exhibits a resonance at −66 ppm and represents a further modest upfield shift of ~16 ppm compared to the monochloro analog **6**, diagnostic of a pentacoordinate Pb complex with a stronger Pb···O interaction.

The crystal structure of **8** illustrates it to be a coordination polymer *via* intermolecular Cl–Pb···Cl units, along with intramolecular Pb···O interaction *trans* to the other, dangling, Cl atom (Fig. 5).

The two independent moieties in the asymmetric unit cell exhibit a slightly distorted octahedral geometry. The intermolecular chain-producing Cl–Pb···Cl interaction exhibits distinctive Pb···Cl bond lengths of 2.676(3) Å for Pb1–Cl2 and 2.944(3) Å for Pb2–Cl2 (and Pb1–Cl4). The presence of two significantly differing Pb–Cl internuclear distances are similar, albeit with significantly greater differences, to those noted

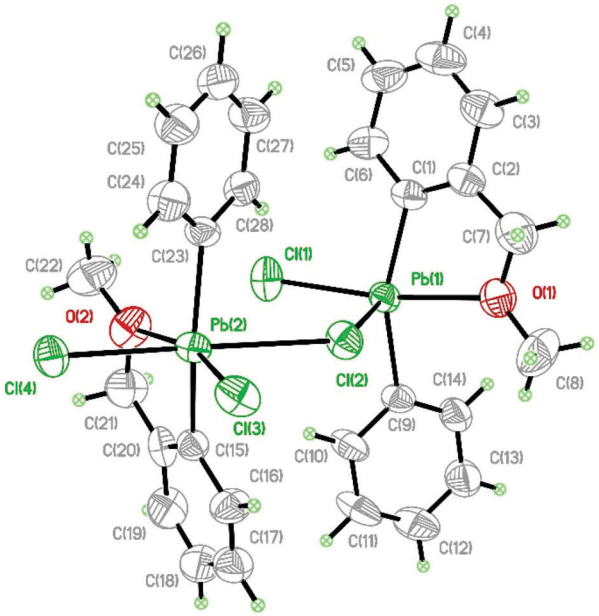

Fig. 5 ORTEP description of the asymmetric unit for **8** (CCDC = 2087427†). Selected bond lengths (Å) and angles (°): O1–Pb1 = 2.520(6), O2–Pb2 = 2.563(6), Pb1–Cl1 = 2.523(3), Pb1–Cl2 = 2.676(3), Pb2–Cl3 = 2.521(3), Pb2–Cl4 = 2.655(3), Pb2–Cl2 = 2.944(3), Pb1–Cl4^1 = 2.944(3), O1–Pb1–Cl1 = 164.5(2), Pb1–O1–C7 = 113.3(6), O2–Pb2–Cl3 = 165.6(2), Pb2–O2–C21 = 112.5(5), Cl2–Pb1–Cl4^1 = 178.8(1), Cl2–Pb2–Cl4 = 178.1(1), Pb1–Cl2–Pb2 = 126.6(1), Pb2–Cl4–Pb1^2 = 128.7(1). References: ^{1} = *x*, *y* + 1, *z*; ^{2} = *x*, *y* − 1, *z*.

above in the distorted TBP structure of Me_3PbCl, 2.814 and 2.764 Å.[30] The bulkier Ph_3PbCl with a similar TBP polymeric structure has the two Pb–Cl internuclear distances equivalent at 2.71 Å,[29] and the published structure of Ph_2PbCl_2,[29] also a coordination polymer, but in which both Cl atoms form intermolecular interactions with Pb, with equivalent Cl–Pb···Cl distances of 2.795 Å. In the structure of **8** an intramolecular Pb···O bond replaces one the bridging Pb–Cl bonds of Ph_2PbCl_2. The two intramolecular Pb···O bond distances (2.520(6) and 2.563(6) Å) are both shorter than in **6** (2.618(4) Å) as expected due to increasing Lewis acidity of the Pb atom bonded to two chlorine atoms. The *trans* dangling Pb–Cl bond distances of 2.523(3) and 2.521(3) Å, respectively are also correspondingly shorter than in **6** (2.555(1) Å).

Chemical studies on dangling arm materials

We have reported the selective alkyl and aryl group transfer from organolead compounds to tin compounds, specifically to tin chlorides.[12] Such reactions can result in an exchange of aryl/alkyl group on Pb for a chlorine on tin, as illustrated in eqn (3):

$$Ph_3PbCl + Me_3SnCl \rightarrow Ph_2PbCl_2 + Me_3SnPh \quad (3)$$

In a preliminary study we have synthesized the chlorinated organolead compounds **6** and **7** described above using this chemistry. Compounds **4** and **5** were dissolved in $CDCl_3$ and

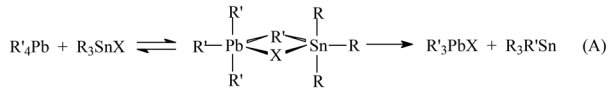

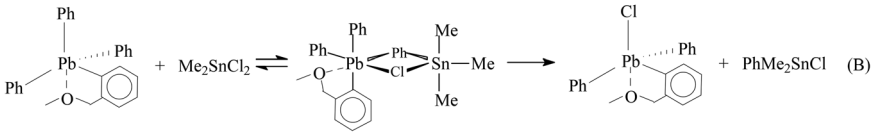

Scheme 2 Possible bridging transition state/intermediate for the exchange processes.

mixed with an equimolar amount of Me_2SnCl_2 in a sealed NMR tube and monitored *via* NMR spectroscopy. The reactions, although slower that those involving Ph_4Pb, produced the expected chlorinated compounds **6** and **7** quantitatively, and selectively, together with the corresponding $PhMe_2SnCl$ (eqn (4)). Typical monitoring of the reaction of **4** and **5** with Me_2SnCl_2 can be observed in the ESI.†

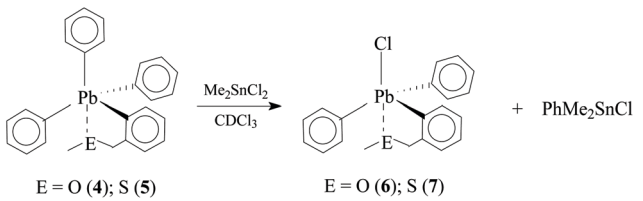

(4)

No evidence for the transfer of the dangling arm aryl group was observed and furthermore, if an excess of Me_2SnCl_2 was added to the reaction no further progression to the di-chloro Pb derivatives was observed.

The slowing of the transfer reaction compared to that of Ph_4Pb supports our prior suggestion that a plausible mechanism involves a bridging transition state/intermediate where the Pb atom exhibits Lewis acid character with respect to an initial interaction with a lone pair of electrons on the chlorine atom bonded to tin, (Scheme 2A). The Lewis acidity of the Pb atom in **4** and **5** is significantly reduced compared to Ph_4Pb, and furthermore a possible a six-coordinate species (Scheme 2B) will have a steric constraint slowing the chemistry.

We have no experimental evidence to back up this mechanistic suggestion but are in the process of applying some quantum mechanical approaches to tease out this or other possibilities.

Conclusions

The new organolead materials reported, $[2\text{-}(CH_3ECH_2)C_6H_4]PbPh_{3-n}Cl_n$, ($n$ = 0, E = O (**4**), E = S (**5**); n = 1, E = O (**6**), E = S (**7**); n = 2, E = O (**8**), are the first to involve intramolecular Pb⋯O(S) secondary bonding. These interactions significantly impact the structure of the compounds, with progressive trigonal bipyramidal geometry observed as the chlorine content increases the Lewis acidity of Pb. The presence of the intramolecular Pb⋯ O(S) bonding has a clear stabilization of the aryl group as noted by the preferential cleavage of the unsubstituted phenyl groups by treatment with HCl, and specific unsubstituted phenyl group transfers to organotin chlorides. We are currently collaborating with Professor Balazs Pinter in performing quantum chemical calculations on these products with respect to their structures, NMR characteristics, and in ascertaining plausible mechanisms for the organic group transfer reaction of organoleads to organotin chlorides. At the suggestion of a referee we also anticipate examining the reactivity of $Ph_{4-n}Cl_nPb$ with various RCH_2EMe materials to possibly observe related intermolecular interactions leading to hypercoordinated materials.

Author contributions

The manuscript was written, reviewed and approved with contributions by all the authors.

Conflicts of interest

There are no conflicts of interest.

Acknowledgements

We are grateful for support of this research by the Welch Foundation (Grant AH-0546). We also acknowledge the Kresge Foundation for a maintenance endowment for upkeep of our NMR facilities and the NSF-MRI Program (Grant CHE-1827875) for purchase of the Venture system.

References

1 C. Lowig, *Liebigs Ann. Chem.*, 1853, **88**, 318–323.
2 C. Lowig, *J. Prakt. Chem.*, 1853, **60**, 304–310.
3 T. Midgley and T. A. Boyd, *J. Ind. Eng. Chem.*, 1922, **14**, 894–898, DOI: 10.1021/ie50154a004.

4 J. T. Pinhey, *Comprehensive Organometallic Chemistry II, Pergamon*, 1995, vol. 11.
5 Y. Yamamoto and J. Yamada, *J. Am. Chem. Soc.*, 1987, **109**, 4395–4396.
6 Y. Yamamoto, J. Yamada and T. Asano, *Tetrahedron*, 1992, **48**, 5587–5596.
7 J. Yamada, H. Abe and Y. Yamamoto, *J. Am. Chem. Soc.*, 1990, **112**, 6118–6120.
8 T. Furuta and Y. Yamamoto, *J. Chem. Soc., Chem. Commun.*, 1992, 863–864.
9 J. T. Pinhey, *Aust. J. Chem.*, 1991, **44**, 1353–1382.
10 H. C. Bell, J. T. Pinhey and S. Sternhell, *Aust. J. Chem.*, 1979, **32**, 1551–1560.
11 D. H. R. Barton, J. P. Finet, C. Giannotti and F. Halley, *J. Chem. Soc., Perkin Trans. 1*, 1987, 241–249.
12 R. N. Arias-Ugarte and K. H. Pannell, *Dalton Trans.*, 2018, **47**, 1703–1708.
13 P. J. Guiry and P. J. McCormack, *Sci. Synth.*, 2003, **5**, 653–663.
14 P. G. Harrison, *Comprehensive Organometallic Chemistry*, Oxford, Pergamon, 1982, vol. 2.
15 O. Mó, M. Yáñez, M. M. Eckert-Maksić, Z. B. Maksić, I. Alkorta and J. Elguero, *J. Phys. Chem. A*, 2005, **109**, 4359–4365.
16 Organochlorine Pesticides – an overview|ScienceDirect Topics https://www.sciencedirect.com/topics/agricultural-and-biological-sciences/organochlorine-pesticides (accessed Aug 8, 2019).
17 (*a*) A. Bauza, S. K. Seth and A. Frontera, *Coord. Chem. Rev.*, 2019, **384**, 107–125; (*b*) D. Sethio, V. Oliveira and E. Kraka, *Molecules*, 2018, **23**, 2763–2784.
18 (*a*) A. Khan and D. Foucher, *Coord. Chem. Rev.*, 2016, **312**, 41–66; (*b*) A. Zickgraf, M. Beuter, U. Kolb, M. Drager, R. Tozer, D. Dakternieks and K. Jurkschat, *Inorg. Chim. Acta*, 1998, **275–276**, 203–214; (*c*) T. Lébl, Z. Petra and C. Bruhn, *Eur. J. Inorg. Chem.*, 2005, 2536–2544; (*d*) D. G. Vargas-Pineda, T. Guardado, F. Cervantes-Lee, A. J. Metta-Magaña and K. H. Pannell, *Inorg. Chem.*, 2010, **49**, 960–968; (*e*) A. Khan, J. Pau, J. Loungxay, T. Magobenny, R. Wylie, R. Stephen, A. J. Lough and D. Foucher, *J. Organomet. Chem.*, 2019, **900**, 1209–1210; (*f*) R. A. Varga, K. Jurkschat and C. Silvestru, *Eur. J. Inorg. Chem.*, 2008, 708–716.
19 U. H. Berlekamp, A. Mix, B. Neumann, H.-G. Stammler and P. Jutzi, *J. Organomet. Chem.*, 2003, **667**, 167–175.
20 R. A. Varga, M. Schuermann and C. Silvestru, *J. Organomet. Chem.*, 2001, **623**, 161–167.
21 T. Munguia, M. López-Cardoso, F. Cervantes-Lee and K. H. Pannell, *Inorg. Chem.*, 2007, **46**, 1305–1314.
22 T. Lebl, A. Smicka, J. Brus and C. Bruhn, *Eur. J. Inorg. Chem.*, 2003, **1**, 143–148.
23 (*a*) D. G. Vargas, A. J. Metta-Magaña, H. K. Sharma, M. M. Whalen, T. M. Gilbert and K. H. Pannell, *Inorg. Chim. Acta*, 2017, **468**, 125–130; (*b*) I. A. Tejeda, R. Maldonado and K. H. Pannell, Paper 025.190 U Therapeutic organotin compounds against Leishmania major and Trypanosoma cruzi, Texas Academy of Science, 2018 Meeting, Midland, TX. https://www.texasacademyofscience.org/assets/PastMeetingPrograms/TAS%20Program%202018.pdf.
24 A. Cristea, A. Silvestru and C. Silvestru, *Stud. Univ. Babes-Bolyai, Chem.*, 2009, **4**, 223–235.
25 (*a*) T. Munguia, I. J. Pavel, R. N. Kapoor, F. Cervantes-Lee, L. Parkanyi and K. H. Pannell, *Can. J. Chem.*, 2003, **81**, 1388–1397; (*b*) M. López-Cardoso, D. G. Vargas-Pineda, P. Román-Bravo, M. E. Rosas-Valdez, A. Ariza-Roldan, R. S. Razo-Hernández, K. H. Pannell and R. Cea-Olivares, *Inorg. Chim. Acta*, 2018, **475**, 28–34; (*c*) H. K. Sharma, A. J. Metta-Magaña, L. Saucedo, M. Lopez-Cardoso and K. H. Pannell, *Tex. J. Sci.*, 2021, **73**, 2, DOI: 10.32011/txjsci_73_1_Article2.
26 (*a*) P. Apodaca, F. Cervantes-Lee and K. H. Pannell, *Main Group Chem.*, 2001, **24**, 597–601; (*b*) T. N. Mitchell and J. G. F. Huber, *J. Chem. Soc., Dalton Trans.*, 1978, **8**, 960–964.
27 L. A. Margolis, C. D. Schaeffer and C. H. Yoder, *Appl. Organomet. Chem.*, 2003, **17**, 236–238.
28 H. K. Sharma, R. J. Villazana, F. Cervantes-Lee, L. Párkányi and K. H. Pannell, *Phosphorus, Sulfur Silicon Relat. Elem.*, 1994, **87**, 257–266.
29 M. Mammi, V. Busetti and A. Del Pra, *Inorg. Chim. Acta*, 1967, **1**, 419–423.
30 D. Zhang, S.-Q. Dou and A. Weiss, *Z. Naturforsch., A: Phys. Sci.*, 1991, **46**, 337–343.